Accurate Band Gaps for Semiconductors from Density Functional Theory

3 AUTHORS:

Hai Xiao
California Institute of Technology
20 PUBLICATIONS **233** CITATIONS

SEE PROFILE

Jamil Tahir-Kheli
California Institute of Technology
35 PUBLICATIONS **1,685** CITATIONS

SEE PROFILE

William A. Goddard
California Institute of Technology
**1,347** PUBLICATIONS **69,067** CITATIONS

SEE PROFILE

Accurate Band Gaps for Semiconductors from Density Functional Theory

Hai Xiao, Jamil Tahir-Kheli, and William A. Goddard, III*

Materials and Process Simulation Center, MC 139-74, California Institute of Technology, Pasadena, California 91125, United States

ABSTRACT An essential issue in developing semiconductor devices for photovoltaics and thermoelectrics is to design materials with appropriate band gaps plus the proper positioning of dopant levels relative to the bands. Local density (LDA) and generalized gradient approximation (GGA) density functionals generally underestimate band gaps for semiconductors and sometimes incorrectly predict a metal. Hybrid functionals that include some exact Hartree−Fock exchange are known to be better. We show here for $CuInSe_2$, the parent compound of the promising CIGS $Cu(In_xGa_{1-x})Se_2$ solar devices, that LDA and GGA obtain gaps of 0.0−0.01 eV (experiment is 1.04 eV), while the historically first global hybrid functional, B3PW91, is surprisingly better than B3LYP with band gaps of 1.07 and 0.95 eV, respectively. Furthermore, we show that for 27 related binary and ternary semiconductors, B3PW91 predicts gaps with a mean average deviation (MAD) of only 0.09 eV, which is substantially better than all modern hybrid functionals.

SECTION Electron Transport, Optical and Electronic Devices, Hard Matter
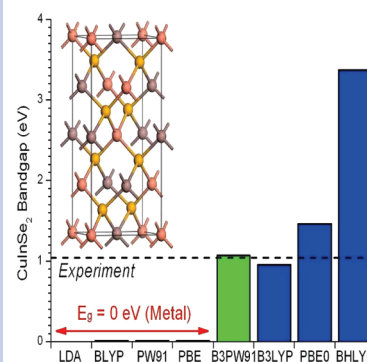
Modern density functional theory (DFT) provides an extremely valuable tool for predicting structures and energetics of new materials for both finite and periodic systems. In theory, the electron affinity and ionization potential can be obtained exactly from the ground-state energy differences of the $N+1$ and $N-1$ electron systems versus the N electron system. In practice, for infinite solids, the band gap (difference between the ionization potential and the electron affinity) is obtained from the difference in the orbital energies of the LUMO (conduction band minimum) and the HOMO (valence band maximum) obtained from a single calculation. It is well documented[1,2] that standard DFT exchange-correlation (XC) functionals [including various generalized gradient approximations (GGA)] dramatically underestimate the band gaps, E_g, for insulators due to the existence of a derivative discontinuity of the energy with respect to the number of electrons.[1] For example, the undoped antiferromagnetic parent compound of cuprate high-temperature superconductors, La_2CuO_4, has a band gap of 2 eV, but LDA, PBE, and PW91 all predict metallic character (no band gap).[3] This failure of pure DFT functionals greatly hampers their applications to superconductors, photovoltaics, and thermoelectric materials, where an accurate description of the band gap and the positions of states at the band edges is essential in designing new materials with improved absorption and transport properties.

It has been known for some time that including some exact Hartree−Fock (HF) exchange in the modern hybrid density functionals[3−6] (B3LYP, PBE0, HSE, etc.) leads to substantially improved band gaps. Here, we show that the historically first hybrid density functional, B3PW91, leads to dramatically better band gaps for the binary and ternary semiconductor compounds that are of interest in photovoltaics and thermoelectrics. This observation and the calculated band gaps for 27 binary and ternary semiconductors relevant to photovoltaics constitute the main results of this paper.

Our motivation in these studies was to study the properties of the $Cu(In_xGa_{1-x})Se_2$ (CIGS) class of solar cells, pioneered by NREL, with efficiencies as high as 19.9 %.[7] The heterojunction in these materials is between n-type CdSe and a p-type alloy of $CuGaSe_2$ and $CuInSe_2$ (with atomic ratios of $Cu/(In + Ga) \approx 0.81$ and $Ga/(In + Ga) \approx 0.30$).[7] The important issues here are the magnitude of the direct band gap and the offsets in the band states at the interfaces as a function of composition. We were disappointed to find that the PBE and PW91 GGAs lead to a band gap for $CuInSe_2$ of $E_g = 0.01$ eV (LDA leads to zero band gap) compared to the experimental value of $E_g = 1.04$ eV. Moreover, the B3LYP hybrid functional (which obtains the correct band gap[3] of 2.0 eV for La_2CuO_4) leads to $E_g = 0.95$ eV, which is too small by 9 %. This led us to explore the performance of other DFT methods.

Here, we report the performance of nine popular XC functionals, including pure and unscreened hybrid functionals, using standard molecular Gaussian-type basis sets for both $CuGaSe_2$ and $CuInSe_2$ bulk systems. We find that B3PW91 leads to a mean average deviation (MAD) of 0.06 eV. This is far more accurate than all other methods (second is B3LYP with MAD = 0.18 eV). To determine the generality of this success, we considered a set of 27 semiconductors with a

Table 1. Calculated Band Gap and Lattice Parameters for $CuInSe_2$ Chalcopyrite Crystal Compared to Experiment[a]

XC	E_g (eV)	error E_g (eV)	HF%	a/Å	c/Å	$\eta = c/2a$	u(Se)	% error volume
exptl.[21]	1.04			5.781	11.642	1.007	0.226	
B3PW91	**1.07**	**0.03**	**20%**	**5.911**	**11.895**	**1.006**	**0.229**	**6.82**
PW91/USPP[22]	0.04	1.00	0%	5.836	11.657	0.999	0.221	2.04
LDA	0.00	1.04	0%	5.787	11.676	1.009	0.216	0.50
BLYP	0.01	1.03	0%	6.057	12.196	1.007	0.224	15.00
PW91	0.01	1.03	0%	5.929	11.953	1.008	0.221	8.00
PBE	0.01	1.03	0%	5.935	11.965	1.008	0.222	8.32
B3LYP	0.95	0.09	20%	5.998	12.046	1.004	0.232	11.38
PBE0	1.46	0.42	25%	5.892	11.857	1.006	0.230	5.80
BHLYP	3.37	2.33	50%	5.982	11.945	0.998	0.240	9.86

[a] B3PW91 (bold) leads to the most accurate band gap (3 times better than B3LYP and 99 times better than PBE or PW91). Here, η is the tetragonal distortion, and u(Se) is the internal relaxation. HF exchange (HF%) is clearly important but at the right level (~20%).

Table 2. Calculated Band Gap and Lattice Parameters for $CuGaSe_2$ Chalcopyrite Crystal Compared to Experiment[a]

XC	E_g (eV)	error E_g (eV)	HF%	a/Å	c/Å	$\eta = c/2a$	u(Se)	% error volume
exptl.[23]	1.67			5.614	11.022	0.982	0.259	
B3PW91	**1.58**	**0.09**	**20%**	**5.729**	**11.234**	**0.981**	**0.255**	**6.14**
PW91/USPP[22]	0.14	1.53	0%	5.609	11.147	0.994	0.244	0.95
LDA	0.24	1.43	0%	5.589	11.135	0.996	0.243	0.13
BLYP	0.02	1.65	0%	5.852	11.589	0.990	0.250	14.25
PW91	0.10	1.57	0%	5.729	11.358	0.991	0.248	7.31
PBE	0.10	1.57	0%	5.735	11.366	0.991	0.248	7.61
B3LYP	1.40	0.27	20%	5.812	11.371	0.978	0.257	10.57
PBE0	2.02	0.35	25%	5.714	11.184	0.979	0.255	5.12
BHLYP	3.96	2.29	50%	5.810	11.206	0.964	0.265	8.89

[a] B3PW91 (bold) leads to the most accurate lattice parameters and band gap (3 times better than B3LYP and 17 times better than PBE or PW91). Other columns are as those in Table 1.

focus on ternary compounds having the chalcopyrite structure relevant to photovoltaic applications. We find that B3PW91 leads to remarkable accuracy, with MAD = 0.09 eV for band gaps and 2.2% for lattice parameters. For all cases considered here, the band gaps are found to be direct (HOMO and LUMO at the same k-vector).

In order to determine whether any of the common methods for DFT could provide sufficient accuracy, we considered a series of XC functionals for band calculations on the $CuInSe_2$ and $CuGaSe_2$ chalcopyrite crystals. This included:

- Simple local density approximation (LDA): SVWN[8,9]
- Generalized gradient approximation (GGA): BLYP,[10,11] PW91,[12] PBE[13]
- Hybrid methods (GGA plus exact exchange): B3PW91,[14] B3LYP,[15] PBE0,[16] and BHLYP.[17]

Tables 1 and 2 show that the original hybrid scheme of Becke, B3PW91, leads to the lowest errors in the band gaps, with a gap that is 0.03 eV too large for $CuInSe_2$ and 0.09 eV too small for $CuGaSe_2$. The B3PW91 band structures and density of states are shown in Figures S1 and S2 of the Supporting Information (SI). In contrast, LDA leads to a zero band gap for $CuInSe_2$, while the GGA methods (PW91, PBE, and BLYP) lead to a gap of only 0.01 eV (99−100% error!). B3LYP leads to too low of a gap by 0.09 eV for $CuInSe_2$ and 0.27 eV for $CuGaSe_2$,

while PBE0 leads to gaps that are too large (by 0.42 eV for $CuInSe_2$ and 0.35 eV for $CuGaSe_2$).

From Tables 1 and 2, we find the following:

(1) The calculated band gaps increase with the percentage of HF exchange, as pointed out by Yang et al.[18] Including exact exchange allows increased localization of the electronic states and is clearly an important factor in obtaining accurate band gaps.

(2) B3PW91 is better than the most popular hybrid functional B3LYP for both lattice parameters and band gaps. Kresse et al.[19] observed this also on metals. The explanation may be that B3LYP underestimates the correlation energy of the uniform electron gas by about 30%, while B3PW91 was designed to be exact for this limit.[20] This suggests that the periodic valence-electron density in a bulk solid is similar to that in a uniform electron gas.

Our PW91 results are comparable to those using plane wave basis sets with an ultrasoft pseudopotential (USPP), validating the accuracy of the Gaussian basis sets used here.

To further evaluate the accuracy of B3PW91 for band gaps of semiconductors, we considered a test set of 27 semiconductors comprised of ternary semiconductors with chalcopyrite structure (currently of great interest for photovoltaic

Table 3. Band Gaps (eV) for 27 Semiconductors[a]

species	exptl.	B3PW91	HSE[6]	species	exptl.	B3PW91	species	exptl.	B3PW91
InP	1.42[24]	1.68	1.64	$CuAlS_2$	3.46[25]	3.47	$AgAlSe_2$	2.55[26]	2.60
InAs	0.41[24]	0.41	0.39	$CuGaS_2$	2.50[27]	2.47	$AgGaSe_2$	1.82[25]	1.65
InSb	0.23[24]	0.30	0.29	$CuInS_2$	1.55[25]	1.60	$AgInSe_2$	1.24[21]	1.24
ZnS	3.84[24]	3.75	3.42	$CuAlSe_2$	2.65[23]	2.55	$CuAlTe_2$	2.06[28]	2.25
ZnSe	2.83[24]	2.73	2.32	$CuGaSe_2$	1.67[23]	1.58	$CuGaTe_2$	1.25[28]	1.34
ZnTe	2.39[24]	2.28	2.19	$CuInSe_2$	1.04[21]	1.07	$CuInTe_2$	1.00[29]	1.14
CdS	2.58[24]	2.55	2.14	$AgAlS_2$	3.60[30]	3.50	$AgAlTe_2$	2.35[31]	2.12
CdSe	1.85[24]	1.84	1.39	$AgGaS_2$	2.70[32]	2.60	$AgGaTe_2$	1.36[31]	1.21
CdTe	1.61[24]	1.67	1.52	$AgInS_2$	1.87[25]	1.87	$AgInTe_2$	1.04[31]	1.09

[a] Experimental references are quoted next to the band gap. B3PW91 leads to MAD = 0.09 eV. Results are also shown using the HSE[6] functional where available, which leads to MAD = 0.27 eV.

Table 4. Lattice Parameters (in Å) for Nine Binary Semiconductors[a]

species	exptl.	B3PW91	HSE[6]	species	exptl.	B3PW91	HSE[6]	species	exptl.	B3PW91	HSE[6]
InP	5.869	5.944	5.909	ZnS	5.345	5.458	5.432	CdS	5.811	5.933	5.896
InAs	6.058	6.159	6.120	ZnSe	5.669	5.754	5.707	CdSe	6.077	6.217	6.152
InSb	6.479	6.584	6.535	ZnTe	6.103	6.212	6.150	CdTe	6.483	6.643	6.568

[a] B3PW91 leads to MAD = 1.9 %; HSE leads to MAD = 1.1 %.

applications) and some binary semiconductors with the zinc blende structure (such as CdS) that are also important solar cell materials. Note that our test set considers only direct band gap semiconductors.

The results are shown in Table 3. We see that B3PW91 yields a MAD = 0.09 eV for band gaps. Moreover, Tables 4 and 5 show that B3PW91 leads to accurate lattice parameters, with MAD = 2.2 %. Generally, B3PW91 is better than B3LYP, which gives MAD = 0.19 eV for band gaps and MAD = 3.4 % for lattice parameters (Tables S1, S2, and S3 in SI).

The one-particle Hamiltonian for the HF method includes a negative exchange self-exchange term that exactly cancels the extra self-repulsion included in the electrostatic potential derived from the density (Poisson equation). However, for the unoccupied orbitals, there is no cancellation leading to energy gaps for molecules that are far too large.

In the LDA and GGA forms of DFT, the HOMO–LUMO gap equals the difference in the first derivatives of total energy with respect to the number of electrons, assuming that the total energy is a straight line between the states with unity and zero occupation.[33] However, Yang et al.[18] showed that an error $\Delta_{straight}$ emerges when the approximate XC functional does not lead to the straight line behavior, so that pure DFT XC functionals such as LDA and GGA generally give $\Delta_{straight} < 0$. They label this as a delocalization error, leading to an underestimation of the band gaps. In contrast, HF leads to $\Delta_{straight} > 0$ (a localization error) and hence an overestimate of band gaps.

In this view, the hybrid functional schemes,[14] containing an average between pure XC functionals and exact HF exchange, might lead to some cancellation between the delocalization and localization errors, which would improve the predicted band gaps (climbing "Jacob's ladder"[34]).

Prior calculations[3–6] have shown that the incorporation of (screened or unscreened) HF exchange can improve the accuracy of DFT band gaps. The most prominent success is from the screened hybrid functional of Heyd–Scuseria–Ernzerhof (HSE).[35] HSE is a screened exchange hybrid functional derived from the PBE0 hybrid DFT functional (which includes 25 % HF exchange). To validate HSE, Scuseria et al.[6] proposed the SC/40 test set of unary and binary compounds. They showed that the HSE functional gives MAD = 0.26 eV over the SC/40 set. They rationalized this increased accuracy by comparison with results from time-dependent DFT (TDDFT) calculations.[36]

Among the SC/40 set are nine binary semiconductors that are also in our test set. Comparing HSE and B3PW91 for this set, we find that B3PW91 leads to MAD = 0.08 eV, which is significantly better than the MAD = 0.27 eV from HSE.[6] It appears that the HSE screening of long-range HF exchange reduces the 25 % HF in PBE0 to something approaching the hybrid level of 20 % HF in B3PW91, which probably provides a better mixing ratio. A complication with HSE is that the screening parameter is generally system-dependent.[36] Thus, in HSE, additional effort must be made to hunt for the optimum choice for each specific system. With B3PW91, no such system-dependent parameters are used.

In summary, we show that the B3PW91 hybrid functional provides accurate band gap predictions for semiconductors (MAD ≈ 0.09 eV) while also leading to accurate lattice parameters. Thus, we recommend B3PW91 combined with standard molecular Gaussian-type basis sets as a practical choice for investigating electronic structures in semiconductor devices. This should provide the basis for more accurate predictions of band offsets at semiconductor interfaces and more accurate positioning of impurity levels in the band gaps

Table 5. Lattice Parameter Results for 18 Ternary Semiconductors (X = S, Se, Te)[a]

	exptl.				B3PW91				
species	a (Å)	c (Å)	$\eta = c/2a$	$u(X)$	a (Å)	c (Å)	$\eta = c/2a$	$u(X)$	% error volume
CuAlS$_2$	5.334	10.444	0.979	0.268	5.388	10.545	0.979	0.264	3.02
CuGaS$_2$	5.347	10.474	0.979	0.254	5.412	10.602	0.979	0.258	3.70
CuInS$_2$	5.523	11.133	1.008	0.229	5.600	11.304	1.009	0.230	4.39
CuAlSe$_2$	5.606	10.901	0.972	0.257	5.711	11.162	0.977	0.260	6.27
CuGaSe$_2$	5.614	11.022	0.982	0.259	5.729	11.234	0.981	0.255	6.14
CuInSe$_2$	5.781	11.642	1.007	0.226	5.909	11.899	1.007	0.229	6.78
AgAlS$_2$	5.695	10.260	0.901	0.300	5.819	10.400	0.894	0.299	5.83
AgGaS$_2$	5.757	10.304	0.895	0.291	5.839	10.511	0.900	0.294	4.94
AgInS$_2$	5.876	11.201	0.953	0.264	5.983	11.452	0.957	0.267	6.00
AgAlSe$_2$	5.956	10.750	0.902	0.270	6.105	11.059	0.906	0.291	8.09
AgGaSe$_2$	5.992	10.883	0.908	0.288	6.121	11.141	0.910	0.286	6.83
AgInSe$_2$	6.104	11.712	0.959	0.258	6.263	12.036	0.961	0.262	8.19
CuAlTe$_2$	5.976	11.804	0.988	0.250	6.158	12.172	0.988	0.247	9.49
CuGaTe$_2$	6.023	11.940	0.991	0.256	6.150	12.197	0.992	0.245	6.51
CuInTe$_2$	6.194	12.416	1.002	0.222	6.340	12.714	1.003	0.223	7.28
AgAlTe$_2$	6.296	11.830	0.939	0.260	6.475	12.257	0.947	0.273	9.58
AgGaTe$_2$	6.288	11.940	0.949	0.260	6.469	12.284	0.950	0.271	8.89
AgInTe$_2$	6.467	12.633	0.977	0.262	6.623	12.988	0.981	0.250	7.83

[a] The MAD for B3PW91 is 2.2%.

for design of photovoltaic, thermoelectric, and other new semiconductor systems.

COMPUTATIONAL DETAILS

All calculations were performed using the CRYSTAL06 package,[37] which employs atomic Gaussian-type basis sets for periodic systems. This simplifies the evaluation of HF exchange. Many codes for periodic bulk calculations use plane wave basis sets, but this greatly complicates the evaluation of HF exchange, and current programs for evaluating HF exchange using plane wave basis sets are computationally expensive.

We used an angular-momentum-projected norm-conserving small-core nonlocal effective core potential[38−42] (ECP) to replace the core electrons. Thus, the neutral Cu atom was described with 19 explicit electrons (two 3s, six 3p, ten 3d, and one 4s in the ground state). The Gaussian basis functions were contracted to the double-ζ plus polarization level from calculations on the most stable unit cell of the pure elements. All calculations included scalar relativistic effects implicitly incorporated through the ECP. We do not include spin−orbit coupling, which can be important in determining band gaps for heavier systems.[43,44] Thus, our band gaps average over the spin−orbit levels. Specifically, for Cu, Ag, Zn, Cd, Ga, and In, we used the SBKJC small core ECP with double-ζ basis sets[45]; for As and Sb, we used the Stuttgart small core ECP[46] with cc-pVDZ basis sets[47]; for Al, P and S, we used the 6-31Gd basis sets; and for Se and Te, we used the SBKJC large core ECP with double-ζ basis sets[45] augmented by one d polarization function.[48]

All basis sets were modified slightly by setting any exponents more diffuse than 0.10 to this value. This is necessary in order to minimize linear dependency and improve numerical instability for crystalline calculations using CRYSTAL.

For optimizing bulk structures, we used an $8 \times 8 \times 8$ k-point grid. To compute the band structure and density of states, we used $16 \times 16 \times 16$ k points on the optimized structure.

SUPPORTING INFORMATION AVAILABLE The B3PW91 calculated band structures, density of states for CuGaSe$_2$ and CuInSe$_2$, and the performance of B3LYP over the test set are included here. This material is available free of charge via the Internet at http://pubs.acs.org.

AUTHOR INFORMATION

Corresponding Author:
*To whom correspondence should be addressed. E-mail: wag@wag.caltech.edu.

REFERENCES

(1) Perdew, J. P.; Levy, M. Physical Content of the Exact Kohn−Sham Orbital Energies: Band Gaps and Derivative Discontinuities. *Phys. Rev. Lett.* **1983,** *51*, 1884–1887.

(2) Sham, L. J.; Schlüter, M. Density-Functional Theory of the Energy Gap. *Phys. Rev. Lett.* **1983,** *51*, 1888–1891.

(3) Perry, J. K.; Tahir-Kheli, J.; Goddard, W. A., III. Antiferromagnetic Band Structure of La$_2$CuO$_4$: Becke-3−Lee-Yang-Parr Calculations. *Phys. Rev. B* **2001,** *63*, 144510.

(4) Seidl, A.; Görling, A.; Vogl, P.; Majewski, J. A.; Levy, M. Generalized Kohn-Sham Schemes and the Band-Gap Problem. *Phys. Rev. B* **1996,** *53*, 3764–3774.

(5) Muscat, J.; Wander, A.; Harrison, N. M. On the Prediction of Band Gaps from Hybrid Functional Theory. *Chem. Phys. Lett.* **2001,** *342*, 397–401.

(6) Heyd, J.; Peralta, J. E.; Scuseria, G. E.; Martin, R. L. Energy Band Gaps and Lattice Parameters Evaluated with the Heyd—Scuseria—Ernzerhof Screened Hybrid Functional. *J. Chem. Phys.* **2005,** *123,* 174101.

(7) Repins, I.; Contreras, M. A.; Egaas, B.; DeHart, C.; Scharf, J.; Perkins, C. L.; To, B.; Noufi, R. 19.9%-Efficient ZnO/CdS/CuInGaSe$_2$ Solar Cell with 81.2% Fill Factor. *Prog. Photovoltaics* **2008,** *16,* 235–239.

(8) Slater, C. J. *Quantum Theory of Molecules and Solids*; McGraw-Hill: New York, 1974; Vol. 4.

(9) Vosko, S. H.; Wilk, L.; Nusair, M. Accurate Spin-Dependent Electron Liquid Correlation Energies for Local Spin Density Calculations: A Critical Analysis. *Can. J. Phys.* **1980,** *58,* 1200–1211.

(10) Becke, A. D. Density-Functional Exchange-Energy Approximation with Correct Asymptotic Behavior. *Phys. Rev. A* **1988,** *38,* 3098–3100.

(11) Lee, C.; Yang, W.; Parr, R. G. Development of the Colle—Salvetti Correlation-Energy Formula into a Functional of the Electron Density. *Phys. Rev. B* **1988,** *37,* 785–789.

(12) (a) Perdew, J. P.; Chevary, J. A.; Vosko, S. H.; Jackson, K. A.; Pederson, M. R.; Singh, D. J.; Fiolhais, C. Atoms, Molecules, Solids, and Surfaces: Applications of the Generalized Gradient Approximation for Exchange and Correlation. *Phys. Rev. B* **1992,** *46,* 6671–6687. (b) Perdew, J. P.; Chevary, J. A.; Vosko, S. H.; Jackson, K. A.; Pederson, M. R.; Singh, D. J.; Fiolhais, C. Erratum. *Phys. Rev. B* **1993,** *48,* 4978.

(13) (a) Perdew, J. P.; Burke, K.; Ernzerhof, M. Generalized Gradient Approximation Made Simple. *Phys. Rev. Lett.* **1996,** *77,* 3865–3868. (b) Perdew, J. P.; Burke, K.; Ernzerhof, M. Erratum. *Phys. Rev. Lett.* **1997,** *78,* 1396.

(14) Becke, A. D. Density-Functional Thermochemistry. III. The Role of Exact Exchange. *J. Chem. Phys.* **1993,** *98,* 5648–5652.

(15) Stephens, P. J.; Devlin, F. J.; Chabalowski, C. F.; Frisch, M. J. Ab Initio Calculation of Vibrational Absorption and Circular Dichroism Spectra Using Density Functional Force Fields. *J. Phys. Chem.* **1994,** *98,* 11623–11627.

(16) Adamo, C.; Barone, V. Toward Reliable Density Functional Methods without Adjustable Parameters: The PBE0 Model. *J. Chem. Phys.* **1999,** *110,* 6158–6170.

(17) Becke, A. D. A New Mixing of Hartree—Fock and Local Density-Functional Theories. *J. Chem. Phys.* **1993,** *98,* 1372–1377.

(18) Mori-Sánchez, P.; Cohen, A. J.; Yang, W. Localization and Delocalization Errors in Density Functional Theory and Implications for Band-Gap Prediction. *Phys. Rev. Lett.* **2008,** *100,* 146401.

(19) Paier, J.; Marsman, M.; Kresse, G. Why Does the B3LYP Hybrid Functional Fail for Metals? *J. Chem. Phys.* **2007,** *127,* 024103.

(20) Perdew, J. P.; Ruzsinszky, A.; Tao, J.; Staroverov, V. N.; Scuseria, G. E.; Csonka, G. I. Prescription for the Design and Selection of Density Functional Approximations: More Constraint Satisfaction with Fewer Fits. *J. Chem. Phys.* **2005,** *123,* 062201.

(21) Shay, J. L; Tell, B.; Kasper, R. M.; Schiavone, L. M. Electronic Structure of AgInSe$_2$ and CuInSe$_2$. *Phys. Rev. B* **1973,** *7,* 4485–4490.

(22) Maeda, T.; Takeichi, T.; Wada, T. Systematic Studies on Electronic Structures of CuInSe$_2$ and the Other Chalcopyrite Related Compounds by First Principles Calculations. *Phys. Status Solidi A* **2006,** *203,* 2634–2638.

(23) Shirakata, S.; Chichibu, S.; Isomura, S. Room-Temperature Photorefiectance of CuAl$_x$Ga$_{1-x}$Se$_2$ Alloys. *Jpn. J. Appl. Phys.* **1997,** *36,* 7160–7161.

(24) Pässler, R. Parameter Sets Due to Fittings of the Temperature Dependencies of Fundamental Bandgaps in Semiconductors. *Phys. Status Solidi B* **1999,** *216,* 975–1007.

(25) Shay, J. L.; Tell, B.; Kasper, H. M.; Schiavone, L. M. p—d Hybridization of the Valence Bands of I—III—VI$_2$ Compounds. *Phys. Rev. B* **1972,** *5,* 5003–5005.

(26) Honeyman, W. N.; Wilkinson, K. H. Growth and Properties of Single Crystals of group I—III—VI$_2$ Ternary Semiconductors. *J. Phys. D: Appl. Phys.* **1971,** *4,* 1182–1185.

(27) Horinaka, H.; Yamamoto, N.; Miyauchi, T. Application of Modulated Phase-Shift-Difference Method with Rotating Quarter-Wave Plate to CuGaS$_2$. *Jpn. J. Appl. Phys.* **1978,** *17,* 521–526.

(28) Bodnar', I. V. CuGaTe$_2$—CuAlTe$_2$ System. *Inorg. Mater.* **2003,** *39,* 10–14.

(29) Quintero, M.; Gonzalez, J.; Woolley, J. C. Optical Energy-Gap Variation and Deformation Potentials in CuInTe$_2$. *J. Appl. Phys.* **1991,** *70,* 1451–1454.

(30) Tsuboi, N.; Hashimoto, Y.; Kurasawa, M.; Kobayashi, S.; Kaneko, F. Preparation and Properties of Ag(Al$_x$Ga$_{1-x}$)S$_2$ Crystals by Iodine Transport Method. *Jpn. J. Appl. Phys.* **1999,** *38,* 6445–6449.

(31) Tell, B.; Shay, J. L.; Kasper, H. M. Some Properties of AgAlTe$_2$ AgGaTe$_2$, and AgInTe$_2$. *Phys. Rev. B* **1974,** *9,* 5203–5208.

(32) Kobayashi, S.; Ohno, T.; Tsuboi, N.; Kaneto, F.; Maruyama, T. Optical Properties near the Fundamental Edge of an AgGaS$_2$ Single Crystal. *Jpn. J. Appl. Phys.* **1989,** *28,* 189–194.

(33) Cohen, A. J.; Mori-Sánchez, P.; Yang, W. Fractional Charge Perspective on the Band Gap in Density-functional Theory. *Phys. Rev. B* **2008,** *77,* 115213.

(34) Perdew, J. P. Schmidt, K. In *Density Functional Theory and Its Application to Materials*; Van Doren, V., Van Alsenoy, C., Geerlings, P., Eds.; AIP: Melville, NY, 2001.

(35) (a) Heyd, J.; Scuseria, G. E.; Ernzerhof, M. Hybrid Functionals Based on a Screened Coulomb Potential. *J. Chem. Phys.* **2003,** *118,* 8207–8215. (b) Heyd, J.; Scuseria, G. E.; Ernzerhof, M. Erratum. *J. Chem. Phys.* **2006,** *124,* 219906.

(36) Brothers, E. N.; Izmaylov, A. F.; Normand, J. O.; Barone, V.; Scuseria, G. E. Accurate Solid-State Band Gaps via Screened Hybrid Electronic Structure Calculations. *J. Chem. Phys.* **2008,** *129,* 011102.

(37) Dovesi, R.; Saunders, V. R.; Roetti, C.; Orlando, R.; Zicovich-Wilson, C. M.; Pascale, F.; Civalleri, B.; Doll, K.; Harrison, N. M.; Bush, I. J.; et al. *CRYSTAL06 User's Manual*; University of Torino: Torino, Italy, 2006.

(38) Goddard, W. A. New Foundation for the Use of Pseudopotentials in Metals. *Phys. Rev.* **1968,** *174,* 659–662.

(39) Melius, C. F.; Goddard, W. A. Ab Initio Effective Potentials for Use in Molecular Quantum Mechanics. *Phys. Rev. A* **1974,** *10,* 1528–1540.

(40) Melius, C. F.; Olafson, B. D.; Goddard, W. A. Fe and Ni Ab Initio Effective Potentials for Use in Molecular Calculations. *Chem. Phys. Lett.* **1974,** *28,* 457–462.

(41) Redondo, A.; Goddard, W. A.; McGill, T. C. Ab Initio Effective Potentials for Silicon. *Phys. Rev. B* **1977,** *15,* 5038–5048.

(42) Hamann, D. R. Generalized Norm-Conserving Pseudopotentials. *Phys. Rev. B* **1989,** *40,* 2980–2987.

(43) Peralta, J. E.; Heyd, J.; Scuseria, G. E. Spin—Orbit Splittings and Energy Band Gaps Calculated with the Heyd—Scuseria—Ernzerhof Screened Hybrid Functional. *Phys. Rev. B* **2006,** *74,* 073101.

(44) Kim, Y.-S.; Hummer, K.; Kresse, G. Accurate Band Structures and Effective Masses for InP, InAs, and InSb Using Hybrid Functionals. *Phys. Rev. B* **2009,** *80,* 035203.

(45) Stevens, W. J.; Krauss, M.; Basch, H.; Jasien, P. G. Relativistic Compact Effective Potentials and Efficient, Shared-Exponent Basis Sets for the Third-, Fourth-, and Fifth-Row Atoms. *Can. J. Chem.* **1992,** *70*, 612–630.

(46) Metz, B.; Stoll, H.; Dolg, M. Small-Core Multiconfiguration-Dirac–Hartree–Fock-Adjusted Pseudopotentials for Post-d Main Group Elements: Application to PbH and PbO. *J. Chem. Phys.* **2000,** *113*, 2563–2569.

(47) Peterson, K. A. Systematically Convergent Basis Sets with Relativistic Pseudopotentials. I. Correlation Consistent Basis Sets for the Post-d Group 13–15 Elements. *J. Chem. Phys.* **2003,** *119*, 11099–11112.

(48) Labello, N. P.; Ferreira, A. M.; Kurtz, H. A. An Augmented Effective Core Potential Basis Set for the Calculation of Molecular Polarizabilities. *J. Comput. Chem.* **2005,** *26*, 1464–1471.